# Reverse microemulsion synthesis of layered gadolinium hydroxide nanoparticles

Yadong Xu,[a] Jugal Suthar,[a] Raphael Egbu,[a] Andrew J. Weston,[a] Andrew M. Fogg,[b]* and Gareth R. Williams[a]*

[a] UCL School of Pharmacy, University College London, London, WC1N 1AX, UK

[b] Department of Chemical Engineering, University of Chester, Thornton Science Park, Cheshire, CH2 4NU, UK

* Authors for correspondence. Email: a.fogg@chester.ac.uk (AMF); g.williams@ucl.ac.uk (GRW). Tel: +44 (0) 1244 512516 (AMF); +44(0) 207 753 5868 (GRW)

## Abstract

A reverse microemulsion approach has been explored for the synthesis of layered gadolinium hydroxide (LGdH) nanoparticles in this work. This method uses oleylamine as a multifunctional agent, acting as surfactant, oil phase and base. 1-butanol is additionally used as a co-surfactant. A systematic study of the key reaction parameters was undertaken, including the volume ratio of surfactant (oleylamine) to water, the reaction time, synthesis temperature, and the amount of co-surfactant (1-butanol) added. It proved possible to obtain pristine LGdH materials at temperatures of 120 °C or below with an oleylamine : water ratio of 1:4. Using larger amounts of surfactant or higher temperatures caused the formation of $Gd(OH)_3$, either as the sole product or as a major impurity phase. The LGdH particles produced have sizes of ca. 200 nm, with this size being largely independent of temperature or reaction time. Adjusting the amount of 1-butanol co-surfactant added permits the size to be varied between 200 and 300 nm.

## Keywords

Layered gadolinium hydroxide; reverse microemulsion; nanoparticles; oleylamine

# 1. Introduction

Ion-exchangeable layered materials have attracted widespread attention for a broad range of applications. Materials able to exchange both cations and anions are known [1], with the latter having been more widely studied [2, 3]. In both cases, the incorporation of guest ions into the interlayer space of the host materials can have a number of benefits: for instance, the stability of guest species can be improved by intercalation [4, 5].

One family of materials which has been particularly extensively studied is the layered double hydroxides (LDHs) [2]. LDHs comprise positively-charged mixed-metal hydroxide layers, with charge-balancing anions in the interlayer region [2]. A large variety of inorganic and organic anions can be incorporated into their interlayer space by ion-exchange reactions [6-8]. This rich intercalation chemistry has been extensively exploited: LDHs have been investigated for applications such as flame retardants [9, 10], catalysts and catalyst precursors [11], $CO_2$ adsorbents [12-16], cement additives [17] and drug delivery systems [7, 18-20]. Bioactive molecules have been intercalated into the interlayer space of LDHs on a number of occasions. Examples include non-steroidal anti-inflammatory drugs such as naproxen, diclofenac, gemfibrozil, ibuprofen and 2-propylpenpenoic acid [7, 19]. There are also reports of the encapsulation of anticancer drugs (e.g. 5-fluorouracil and methotrexate) [21, 22]. LDH-drug intercalates have been found to lead to sustained drug release profiles and reduced side effects compared to the free drug [7, 19].

Beyond LDHs, there exists a range of alternative layered materials capable of anion exchange. These include the recently reported layered rare-earth hydroxides (LRHs). There are a range of LRHs possible, but those capable of anion exchange have the general formula $[R_2(OH)_5]^+(A^{n-})_{1/n}\cdot yH_2O$ (where R = $Ln^{3+}$, $A^{n-}$ = an anion, and $1 \leq y \leq 2$). LRHs contain lanthanide cations and hydroxide ions in their positively charged layers, and charge-balancing anions in the interlayer region [23-25]. Typical examples include $[Gd_2(OH)_5]Cl\cdot 1.5H_2O$ and $[Yb_2(OH)_5]Cl\cdot 1.5H_2O$ [3]. The inorganic anions typically present in the gallery of LRHs immediately after synthesis can be readily replaced by other inorganic or organic species such as azamacrocyclic crown ether [26], or amino acids [27].

LRHs could thus be potent alternatives to LDHs for use as, for instance, drug delivery systems. Moreover, LRHs possess the magnetic and fluorescent properties of the rare-earth metals they contain, which could give additional benefits. The combination of ion exchange intercalation chemistry and rare earth elements in the layers can lead to integrated materials with many applications in medical science [28, 29], catalysis [30], separation science [26], sensor technologies

[31], and luminescence devices [5, 27, 32-40]. Some studies have focused on incorporating sensitizers or quenchers to tune the colour emission of LRH hybrids, for instance [3, 5, 27].

Magnetic resonance imaging (MRI) is a technique widely used in biomedical imaging. It is popular in part because it does not use radioactive agents or high-energy electromagnetic waves, and has high spatial and temporal resolution [41]. To obtain good quality images, however, the patient must be administered what is termed a "contrast agent", a chemical entity used to enhance the quality of the images obtained and permit accurate diagnoses. Commercial contrast agents are commonly based on $Gd^{3+}$. This is because the electronic relaxation time of $Gd^{3+}$ is very long and it has a high number of unpaired electrons, which means that it can enhance both the longitudinal ($r_1$) and transverse ($r_2$) relaxation times of water protons [42]. Free $Gd^{3+}$ is extremely toxic, and thus the agents used in the clinic are based on chelation complexes designed to ensure that the Gd present remains complexed at all times. An alternative route to preclude free $Gd^{3+}$ getting into solution is to incorporate it into an inorganic matrix, and hence layered gadolinium hydroxides (LGdHs) might be viable contrast agents [43]. The potential of LGdHs in this regard has been explored in several reports [28, 29, 43, 44], and the results obtained are promising. The LGdH matrix has also attracted a little attention for use as a drug delivery system, with the intercalation of several pharmaceutically active molecules including antibiotics, amino acids, and microRNA [43, 45].

Control of particle size can be extremely important to achieve the desired results *in vivo*, and for this reason much attention has been paid in particular to the production of nanoscale materials, which have been explored in many fields [46]. The size of LDH particles has been shown to play an important role in their interactions with cells, for instance [47]. Therefore, controlling the particle size of LGdH will be important to ensure uptake by cells, and thus to improve its performance in MRI applications. However, little effort has been applied to the synthesis of LRH nanoparticles to date.

One route to control particle size is the use of reverse microemulsion systems. These comprise water droplets dispersed in an oil continuous phase; when materials are grown from an aqueous solution, performing the reaction in such systems means that the particle size is controlled by the size of the droplets, so long as that the emulsion is stable and there is no coalescence. This approach has been found to lead to high degrees of control over particle size, morphology, geometry, and surface area [46], and microemulsion systems have emerged as an effective approach to synthesize nanomaterials such as metallic catalysts [48], semiconductors [49], ceramics [50], and silica [51]. Here, we apply this approach for the first time to the synthesis of nanosized LGdH materials, aiming

to produce particles with sizes suitable for cellular uptake. We report the synthesis of LGdH nanoparticles using a method in which oleylamine acts as oil phase, base and surfactant, permitting an extremely simple microemulsion formulation to be employed.

# 2 Experimental

## 2.1 Materials

Oleylamine and 1-butanol were purchased from Sigma-Aldrich (Gillingham, UK), while gadolinium chloride hexahydrate was supplied by Alfa Aesar (Heysham, UK). All water used was deionized, and all other chemicals were of analytical grade and used without further purification.

## 2.2 Methods

### 2.2.1 General protocol

A novel reverse microemulsion method which employs oleylamine as oil phase, base and surfactant was developed in 2012 to synthesize LDHs [47]. Experiments were carried out following this method with minor modifications. A 0.5 M solution of $GdCl_3 \cdot 6H_2O$ in deionized water was first prepared, and to this a mixture of oleylamine and 1-butanol was added dropwise with vigorous stirring. After 10 min of constant stirring, the resultant mixture was transferred to a Telfon-lined stainless steel autoclave (23 mL) and treated hydrothermally. The resulting precipitates were collected by centrifugation, washed with a mixture of water and ethanol (1:1, v/v), and dried at 40 ˚C for one day.

### 2.2.2 Optimization

A detailed optimization process was undertaken in this work. First, since the volume ratio of surfactant to water is known to be a determining factor for particle size [47, 52], a range of oleylamine : water ratios were explored (4:1, 3:2, 1:3 and 1:4). Specifically, 8, 6, 2.5 or 2 mL of oleylamine was first combined with 5 mL of 1-butanol. The resultant mixtures were added to 2, 4, 7.5 or 8 mL of a 0.5 M Gd chloride solution. The total volume of oleylamine and water was kept at 10 mL, and the total solution volume in the autoclave was 15 mL. Hydrothermal treatment was undertaken at 120 ˚C for 18 h. The resulting samples are denoted as LGdH-O*m*-W*n* (*m* = volume of oleylamine, *n*= volume of water).

Second, the temperature was optimized. With an increase in temperature in a hydrothermal process, the particle size of the product tends to be larger [51]; however, high temperatures could also lead to potential degradation or phase transformation. The surfactant to water volume ratio was set to 1:4, and each reaction mixture comprised 2 mL oleylamine, 5 mL 1-butanol, and 8 mL Gd

chloride solution. Hydrothermal treatments were carried out at temperatures ranging from 90 ˚C to 150˚C for 18 h. The products are denoted LGdH-90˚C, LGdH-120˚C, and LGdH-150˚C.

Third, the aging duration is another factor which could determine the particle size: the longer the crystals grow, the larger they will be. A volume ratio of surfactant to water of 1:4 was used, and again each reaction mixture comprised 2 mL oleylamine, 5 mL 1-butanol, and 8 mL Gd chloride solution. LGdH nanoparticles were prepared with hydrothermal treatment at 12 h, 18 h or 24 h at 120 ˚C. The products were named LGdH-12h, LGdH-18h, and LGdH-24h.

Finally, the co-surfactant amount in water-in-oil microemulsion systems has been reported to have an important effect on particle growth, with nanoparticle size rising with an increasing amount of co-surfactant [51]. Hence, the volume of 1-butanol was varied from 3 to 9 mL. The ratio of surfactant to water was fixed at 1:4, so each reaction mixture comprised 2 mL of oleylamine, 8 mL of Gd chloride solution, and between 3 and 9 mL of 1-butanol. Experiments were carried out at 120 ˚C for 12 h. The materials obtained were designated LGdH-3mL, LGdH-5mL, LGdH-7mL and LGdH-9mL.

## 2.3 Characterization

### 2.3.1 X-ray diffraction (XRD)

Power XRD patterns were recorded over the 2θ range from 3 to 45° on a Rigaku MiniFlex 600 diffractometer (Tokyo, Japan), using Cu Kα radiation (λ = 1.5418 Å) at 40 kV and 15 mA.

### 2.3.2 Fourier transform infrared (FTIR) spectroscopy

Infrared spectra were obtained using a Spectrum 100 FTIR spectrometer (Perkin Elmer, Waltham, MA, USA) over the range 650–4000 $cm^{-1}$ with a resolution of 2 $cm^{-1}$.

### 2.3.3 Dynamic light scattering (DLS)

Dynamic light scattering measurements were performed on a Zetasizer Nano ZS instrument (Malvern Instruments, Malvern, UK). 1-2 mg of LGdH nanoparticles was suspended in ethanol and sonicated for ca. 15 min prior to measurements.

### 2.3.4 Transmission electron microscopy (TEM)

LGdH nanoparticles (5 mg) were dispersed in ethanol (1 mL), followed by 20 minutes of sonication. A few drops of each suspension were then placed onto a lacey carbon coated copper grid, and ethanol

allowed to evaporate. TEM was performed using a FEI CM120 Bio Twin microscope (Philips, Amsterdam, Netherlands) with an accelerating voltage of 120 kV.

## 3. Results

The synthesis of LGdH nanoparticles was first attempted using a previously explored protocol in which Triton X-100, 2,2,4–trimethylpentane and 1-butanol act as surfactant, oil phase and co-surfactant [53]. However, this method was time-consuming (3 days) and suffered from low yields. In addition, the obtained nanoparticles were of very low crystallinity (ascribed to stacking defects), and had a wide range of sizes (from tens of nanometers to several micrometers). Replacing 1-butanol with propan-2-ol had no significant effect on the findings. This route was thus deemed unsuitable. We then turned to an alternative literature protocol. Wang and O'Hare [47] have reported an approach using oleylamine (Figure 1) as an multi-functional agent which acts as the oil phase, base, and surfactant simultaneously. Alkaline conditions are provided as a result of the amine group, and the amine head group along with its alkyl chain tail acts as a surfactant. This leads to the formation of reverse micelles in a water-in-oil system. 1-butanol was also added as a co-surfactant, separating the oleylamine units and reducing the repulsive forces between the protonated head groups [47]. Wang and O'Hare's oleylamine method was systematically explored for the synthesis of LGdH in this work.

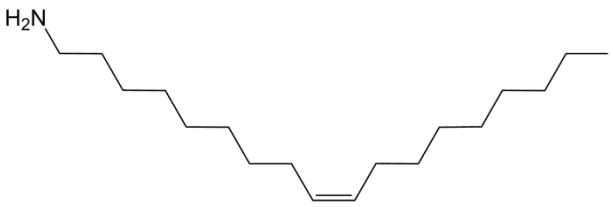


**Figure 1:** The chemical structure of oleylamine.

### 3.1 Effect of surfactant to water ratio

The first reaction parameter to be investigated was the ratio of surfactant to water in the system. A series of emulsions were prepared as detailed in Table 1.

**Table 1:** Details of reactions performed with different ratios of oleylamine to water. All were performed at 120 °C for 18 h, with 5 mL of 1-butanol added.

| Sample ID | Oleylamine volume (mL) | Aqueous solution volume (mL) | Oleylamine/water volume ratio |
|---|---|---|---|
| **LGdH-O8-W2** | 8 | 2 | 4:1 |
| **LGdH-O6-W4** | 6 | 4 | 3:2 |
| **LGdH-O2.5-W7.5** | 2.5 | 7.5 | 1:3 |
| **LGdH-O2-W8** | 2 | 8 | 1:4 |

The powder XRD patterns of the products obtained are presented in Figure 2. Phase-pure LGdH nanoparticles could be synthesized only with a 1:4 volume ratio of oleylamine to water. At ratios below this, the diffraction patterns very closely resemble that of $Gd(OH)_3$ (JCPDS #38-1042). At ratios of 4:1 and 3:2, no lamellar (00*l*) reflections at all were observed in the XRD data. At a volume ratio of 1:3, a weak reflection (marked with an arrow in Figure 2) at ca. 10.5° was observed, which corresponds to the (001) Bragg reflection of LGdH and indicates the presence of a small amount of the LRH alongside the $Gd(OH)_3$ majority product. The pattern obtained for sample LGdH-O2-W8, with a 1:4 ratio of surfactant to water, matches literature data for chloride intercalated LGdH (LGdH-Cl) [54-56]. The position of the (001) Bragg reflection corresponds to an interlayer spacing of 8.48 Å, in excellent agreement with previously reported values for chloride intercalates [28, 56].

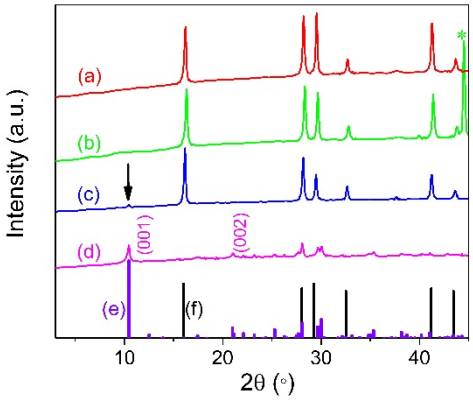


**Figure 2:** Powder X-ray diffraction patterns of LGdH nanoparticles prepared with different volume ratios of surfactant to water: (a) LGdH-O8-W2; (b) LGdH-O6-W4; (c) LGdH-O2.5-W7.5; (d) LGdH-O2-W8. The calculated reflection positions are also shown for (e, purple) LGdH-Cl [56] and (f, black) $Gd(OH)_3$ [JCPDS #38-1042]. The Bragg reflection marked * corresponds to the sample holder.

## 3.2 Effect of temperature

Data for samples prepared at different temperatures with a 1:4 surfactant to water ratio are given in **Figure 3**.

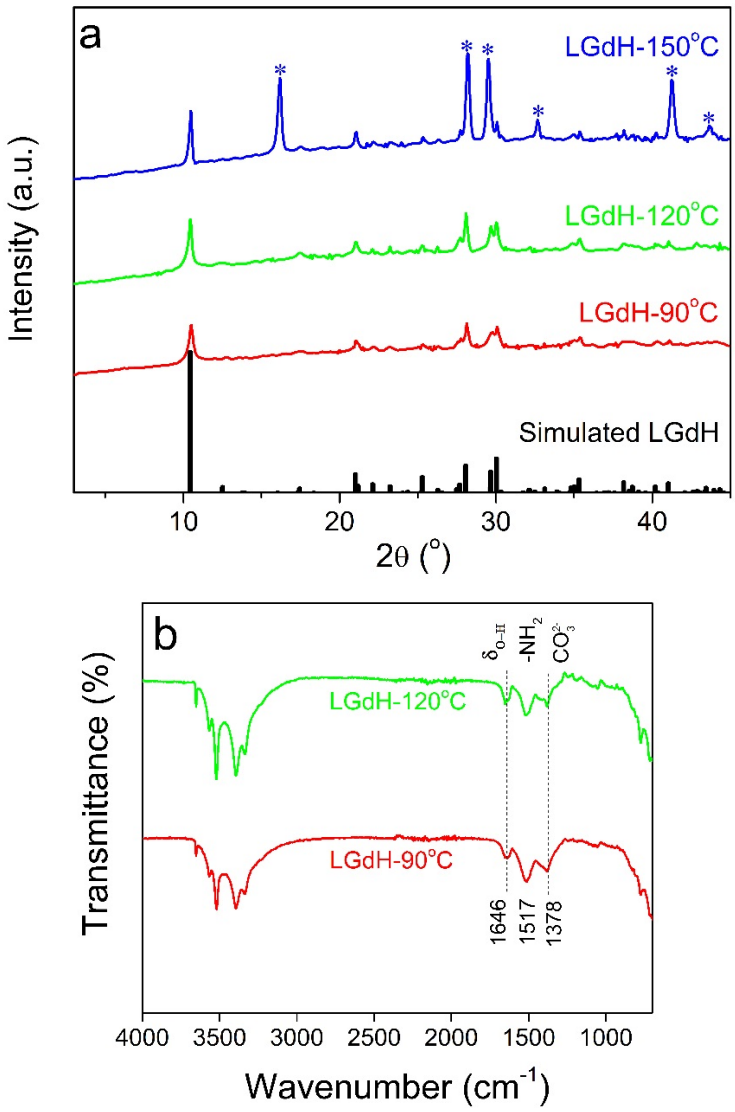


**Figure 3:** Experimental data for syntheses conducted at 90, 120, and 150 °C. (a) XRD patterns; and, (b) IR spectra. Reflections marked with * in (a) arise from $Gd(OH)_3$.

The materials generated at 90, 120 and 150 °C all present basal (00*l*) reflections (Figure 3), indicative of an interlayer spacing of 8.42 Å. Significant amounts of $Gd(OH)_3$ can be seen in the sample synthesized at 150 °C, but phase pure LGdH was successfully synthesized at 90 and 120 °C. The Bragg reflections of product from the 120 °C reaction are somewhat stronger and sharper than those of the 90 °C analogue, implying that samples heated at the higher temperature are better crystallized and have larger crystallite sizes. IR spectra (Figure 3(b)) confirm the successful synthesis of LGdHs at 90 and 120 °C. The two spectra contain the same features, with the broad set of bands centred at ca.

3500 $cm^{-1}$ attributed to the stretching vibration of the OH groups from both interlayer water and the hydroxide layers [26, 40]. The absorbance at 1646 $cm^{-1}$ is ascribed to the bending vibrations of the interlayer water molecules ($\delta_{O-H}$) [57]. Bands below 1000 $cm^{-1}$ correspond to the phonon vibrations of the structure. The peaks at 1517 and 1378 $cm^{-1}$ indicate the presence of residual oleylamine, and of some $CO_3^{2-}$ co-intercalated with the $Cl^-$ anions, respectively.

**Table 2**: Crystallite sizes of LGdH nanoparticles prepared at different temperatures, analyzed using the Scherrer equation (K = 0.89). * denotes occasions where no data could be obtained.

| Sample ID | FWHM (°) | | Crystallite size (nm) | |
|---|---|---|---|---|
| | (001) | (220) | c-direction | ab-plane |
| **LGdH-90°C** | 0.339 | 0.318 | 24.6 | 27.1 |
| **LGdH-120°C** | 0.247 | * | 35.3 | * |

The LGdH patterns can be indexed in orthorhombic symmetry, and hence the (001) Bragg reflection can be applied to estimate the crystallite size along the c-axis (the thickness of the particles), while the (220) reflection can be used to estimate the crystallite size in the ab plane. The values estimated using the Scherrer equation are summarized in Table 2. The crystallite size in the c-direction is found to be around 25 – 35 nm, with a comparable size in the ab-plane where this could be determined. TEM images (**Figure 4**) show both LGdH-90°C and LGdH-120°C to comprise small aggregates of platelets, with lateral sizes between around 100 and 200 nm. The primary particle size is perhaps somewhat larger than the size obtained from Scherrer analysis (as would be expected given the assumptions involved in applying the latter), but overall the two sets of data are consistent.

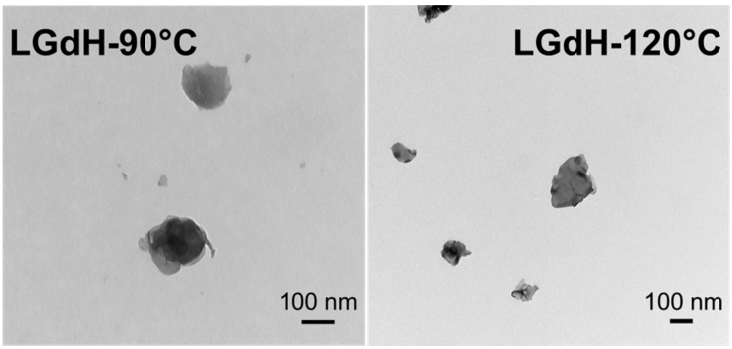


**Figure 4:** TEM images of LGdH prepared at different temperatures.

## 3.3 Effect of time

The volume ratio of oleylamine to water and heating temperature were fixed at 1:4 and 120 °C, while the aging time was varied from 12 to 24 h. XRD patterns of the products are given in **Figure 5**(a). The presence of a series of (00*l*) basal reflections in each case indicates the formation of lamellar structures. The interlayer spacing of all three samples is around 8.45 Å, consistent with the

literature for LGdH-Cl materials [28, 56]. Scherrer analysis of the (001) and (220) reflections (see 120°C.

**Table 3**) reveals that the crystallite size in the ab plane seems to increase with reaction time, but that in the c-diameter is largely constant, with possibly a decrease in size after reaction times longer than 12 h. The IR spectra (**Figure 5**(b)) are analogous to those discussed previously in terms of the peak positions (see discussion of Figure 3(b)).

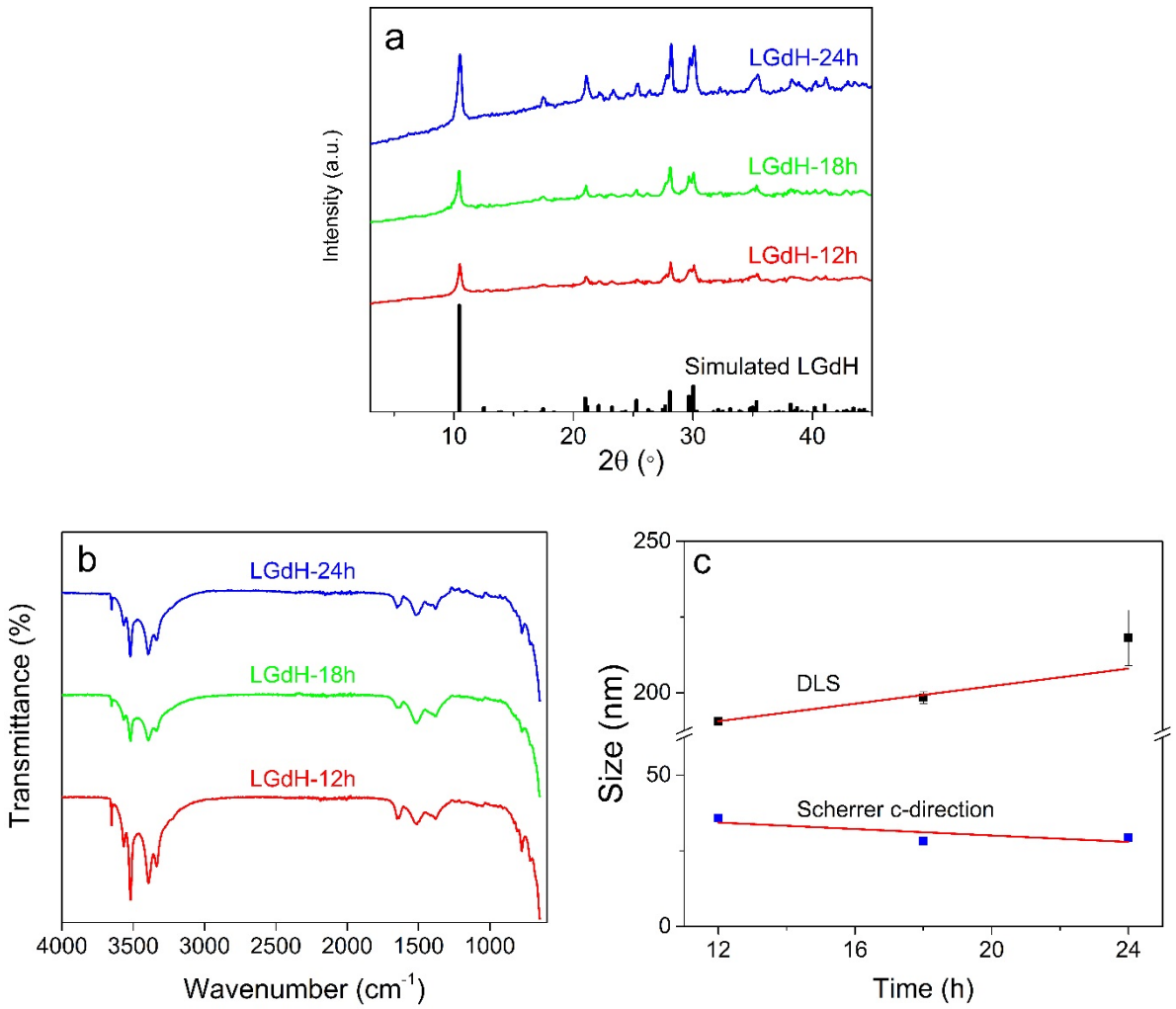


**Figure 5:** Data on the LGdH products obtained after different reaction times. (a) XRD patterns; (b) IR spectra; and, (c) particle size data.

DLS measurements were employed to determine the hydrodynamic particle size (120°C.

**Table 3**). There appears to be a trend to larger particles with longer reaction times (**Figure 5**(c)). TEM data are presented in Figure 6. For each of LGdH-12h, LGdH-18h and LGdH-24h the samples comprise small aggregates of platelets, with sizes roughly in the ranges 250 – 500 nm, 300 – 700 nm, and 250 – 750 nm respectively. These sizes are rather larger than those observed in DLS, which is

ascribed to aggregation occurring during the TEM sample preparation process, but in general support the idea of larger particles forming with increased reaction times. However, the differences observed are slight, and overall it appears that the reaction time has little effect on the particle size.

The LGdH-18h sample was prepared under the same conditions as the LGdH-120°C sample discussed in Section 3.2 and shown in Figure 4. The c-direction crystallite sizes, as determined through the Scherrer equation, are comparable for the two samples (28.2 nm for LGdH-18h, *cf.* 35.3 nm for LGdH-120°C), but the TEM particle sizes are somewhat different. This is ascribed to the propensity of the particles to aggregate, and the presence of different size secondary particles in the different samples imaged. A comparison of Figure 4 and Figure 6 reveals that the primary particle sizes are similar in both, and the DLS particle size for LGdH-18h agrees well with the TEM estimate of particle size for LGdH-120°C.

**Table 3:** Summary of particle size data for LGdH obtained after 12, 18, and 24h. * denotes occasions where no data could be obtained.

| Sample ID | c-direction crystallite size (nm) | ab-plane crystallite size (nm) | DLS hydrodynamic diameter (nm) | |
|---|---|---|---|---|
| | | | Mean | S.D. |
| **LGdH-12h** | 35.8 | * | 191 | 0.4 |
| **LGdH-18h** | 28.2 | 20.2 | 198 | 1.9 |
| **LGdH-24h** | 29.4 | 31.7 | 218 | 9.2 |

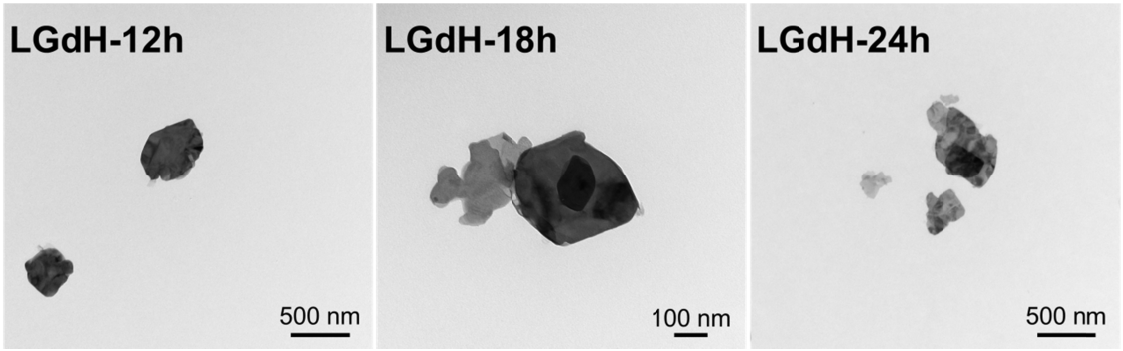


**Figure 6:** TEM images of LGdh-12h, LGdH-18h, and LGdH-24h.

## 3.4 Effect of co-surfactant

The literature reports that the particle size of silica nanospheres prepared by a microemulsion method decreased as the amount of co-surfactant decreased [51]. Therefore, the amount of 1-butanol used in the synthesis was varied in attempts to tune the nanoparticle size. The products' XRD patterns (**Figure 7**(a)) all contain the characteristic basal (00*l*) reflections of layered LGdH particles, with (001) reflections at ca. 10.5° and (002) at ca. 21.1°. The weak reflections between the (001) and (002) reflections indicate the well-ordered in-plane structure of the LGdH materials.

Scherrer analysis of the data (Table 4) does not reveal any clear relationship between the amount of co-surfactant and crystallite size. LGdH-3mL has the largest crystallites in the c-direction, but the non-basal reflections are too broad to permit measurement of their FWHM values. The other three materials have essentially the same crystallite size in the c-direction, and a small amount of variation in the ab plane, with LGdH-7mL presenting the smallest value for the latter.

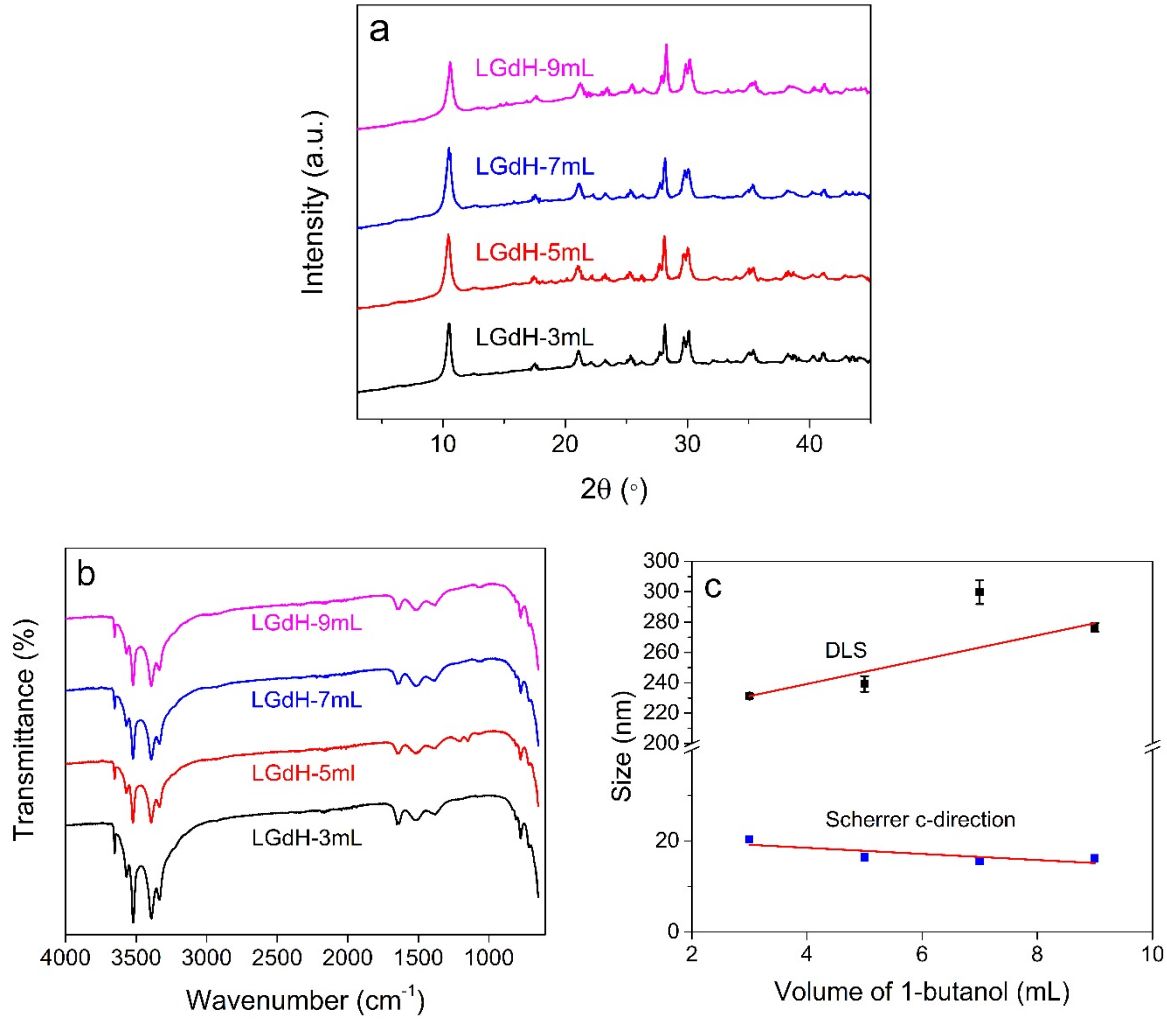


**Figure 7:** The effect of changing the co-surfactant volume on LGdH synthesis. (a) XRD patterns; (b) IR spectra; and, (c) particle size data.

The IR spectra (Figure 7(b)) show the same absorbance peaks as discussed previously, corresponding to -OH, $-NH_2$ and $CO_3^{2-}$ and confirming the formation of LGdH materials. Hydrodynamic diameters were measured by DLS (Table 4), and their relationship with the 1-butanol volume is presented in Figure 7(c). As the amount of co-surfactant increases, there is a general trend for the diameter of the LGdH nanoparticles to increase. This agrees with the literature findings for hollow silica nanoparticles [51]. However, this trend is not completely clear, and it also apparent that there is some batch-to-batch variation in the sizes: LGdH-5mL was prepared under identical synthetic conditions to LGdH-12h, but the two have somewhat different sizes both in terms of XRD

crystallite sizes and DLS particle sizes. Thus, although it seems that using larger amounts of co-surfactant can help to increase the particle size produced a little, this effect is not hugely pronounced. TEM images were obtained on LGdH-3mL and LGdH-5mL (data not shown), and both found to be very similar. The samples comprise aggragrates of platelets, with sizes in the region of 100 – 300 nm.

**Table 4:** Summary of the particle sizes of LGdH obtained with 3, 5, 7, and 9 mL of 1-butanol. * denotes that values could not be obtained.

| Sample ID | c-direction crystallite size (nm) | ab-plane crystallite size (nm) | DLS hydrodynamic diameter (nm) | |
|---|---|---|---|---|
| | | | Mean | S.D. |
| **LGdH-3mL** | 20.4 | * | 231 | 1.5 |
| **LGdH-5mL** | 16.4 | 44.1 | 239 | 5.2 |
| **LGdH-7mL** | 15.6 | 37.3 | 300 | 7.8 |
| **LGdH-9mL** | 16.2 | 47.1 | 277 | 3.0 |

## 4. Discussion

The effect of the surfactant to water ratio [58], reaction temperature, reaction time and the amount of co-surfactant [51] used for the reverse microemulsion synthesis of LGdH have been systematically investigated in this work. We find that the surfactant : water ratio and the reaction temperature must be carefully controlled to ensure that the desired product is formed phase-pure; the use of excessive amounts of surfactant (> 1:4 surfactant : water ratio) or temperatures above 120 °C lead to the formation of $Gd(OH)_3$, either phase-pure or as a major impurity. With a 1:4 ratio and temperatures of 120 °C or below, however, LGdH can be obtained phase-pure. The reaction time and co-surfactant volume have some effect on particle size, but in all cases the sizes are found to be between 200 and 300 nm.

It is reported that as the ratio of surfactant to water increases, the microemulsion droplets tend to become smaller. If the reaction is confined to the aqueous phase, as is the case here, this should lead to smaller particles being generated [46, 58]. LGdH particle size cannot be controlled in this way in the oleylamine/1-butanol system however, because gadolinium hydroxide is found to form with high ratios. Our findings are thus in conflict with the literature on LDH materials [47]. This is because LDHs are typically synthesized at ca. pH 9 – 10, while LGdHs are prepared at ca. pH 6.7 – 7.2 [54, 59]. Oleylamine acts both as base and surfactant, and the transformation of LGdH to $Gd(OH)_3$ presumably arises due to the increasingly strong alkaline environment as the oleylamine content of the system is increased. This problem does not occur with the previously-reported LDH synthesis using oleylamine because of the fact that LDHs are more stable at high pHs. Therefore, the LDH

nanoparticle size can be controlled, and reduced to as little as 49 nm by tuning the surfactant to water volume ratios [47].

## 5. Conclusions

Layered gadolinium hydroxide (LGdH) nanoparticles have been successfully synthesized by employing a novel reverse microemulsion method. Pristine LGdH materials were obtained at temperatures below 150 °C with an oleylamine : water ratio of 1:4. Control of particle size is difficult, however. Attempts to achieve this by using more surfactant and increasing the reaction temperature were unsuccessful because of the propensity of $Gd(OH)_3$ to form. It was found that at 120 °C and below the temperature and the duration of heating have little effect on the size distribution, producing particles around 200 nm. Varying the amount of co-surfactant (1-butanol) used allowed the size to be increased from ca. 200 nm to 300 nm, with use of more butanol giving larger particles. Overall, microemulsions have proved to be an effective and efficient way to synthesized LGdH nanoparticles of 200 – 300 nm in size, but in order to obtain more control over particle size alternative surfactants should be investigated.

## 6. Acknowledgements

The authors gratefully thank Mr David McCarthy and Mrs Kate Keen for assistance with obtaining TEM images. JS and RE thank the EPSRC for the provision of PhD studentships under the Centre for Doctoral Training in Advanced Therapeutics & Nanomedicines (EP/L01646X/1).

## 7. References

[1] M. Ranocchiari, J.A. van Bokhoven, Catalysis by metal–organic frameworks: fundamentals and opportunities, Phys. Chem. Chem. Phys. 13(14) (2011) 6388-6396.

[2] Q. Wang, D. O'Hare, Recent advances in the synthesis and application of layered double hydroxide (LDH) Nanosheets, Chem. Rev. 12 (2012) 4124-4155.

[3] F. Geng, R. Ma, T. Sasaki, Anion-exchangeable layered materials based on rare-earth phosphors: unique combination of rare-earth host and exchangeable anions, Acc. Chem. Res. 43(9) (2010) 1177-1185.

[4] S. Takagi, D.A. Tryk, H. Inoue, Photochemical energy transfer of cationic porphyrin complexes on clay surface, J. Phys. Chem. B 106(21) (2002) 5455-5460.

[5] N. Chu, Y. Sun, Y. Zhao, X. Li, G. Sun, S. Ma, X. Yang, Intercalation of organic sensitisers into layered europium hydroxide and enhanced luminescence property, Dalton Trans 41(24) (2012) 7409-14.

[6] Q. Qin, J. Wang, T. Zhou, Q. Zheng, L. Huang, Y. Zhang, P. Lu, A. Umar, B. Louis, Q. Wang, Impact of organic interlayer anions on the $CO_2$ adsorption performance of Mg-Al layered double hydroxides derived mixed oxides, J. Energy Chem. 26(3) (2017) 346-353.

[7] V. Rives, M. del Arco, C. Martín, Intercalation of drugs in layered double hydroxides and their controlled release: A review, Appl. Clay Sci. 88-89 (2014) 239-269.

[8] G.R. Williams, D. O'Hare, Towards understanding, control and application of layered double hydroxide chemistry, J. Mater. Chem. 16(30) (2006) 3065.

[9] C. Nyambo, P. Songtipya, E. Manias, M.M. Jimenez-Gasco, C.A. Wilkie, Effect of MgAl-layered double hydroxide exchanged with linear alkyl carboxylates on fire-retardancy of PMMA and PS, J. Mater. Chem. 18(40) (2008) 4827-4838.

[10] C. Manzi-Nshuti, J.M. Hossenlopp, C.A. Wilkie, Comparative study on the flammability of polyethylene modified with commercial fire retardants and a zinc aluminum oleate layered double hydroxide, Polym. Degr. Stab. 94(5) (2009) 782-788.

[11] X. Xu, R. Lu, X. Zhao, S. Xu, X. Lei, F. Zhang, D.G. Evans, Fabrication and photocatalytic performance of a $Zn_x Cd_{1-x}S$ solid solution prepared by sulfuration of a single layered double hydroxide precursor, Appl. Catal. B 102(1) (2011) 147-156.

[12] Q. Wang, J. Luo, Z. Zhong, A. Borgna, $CO_2$ capture by solid adsorbents and their applications: current status and new trends, Energy Env. Sci. 4(1) (2011) 42-55.

[13] Q. Wang, H.H. Tay, D.J.W. Ng, L. Chen, Y. Liu, J. Chang, Z. Zhong, J. Luo, A. Borgna, The effect of trivalent cations on the performance of Mg-M-$CO_3$ layered double hydroxides for high‐temperature CO2 capture, ChemSusChem 3(8) (2010) 965-973.

[14] Q. Wang, Z. Wu, H.H. Tay, L. Chen, Y. Liu, J. Chang, Z. Zhong, J. Luo, A. Borgna, High temperature adsorption of $CO_2$ on Mg–Al hydrotalcite: effect of the charge compensating anions and the synthesis pH, Catal. Today 164(1) (2011) 198-203.

[15] Q. Wang, H.H. Tay, Z. Guo, L. Chen, Y. Liu, J. Chang, Z. Zhong, J. Luo, A. Borgna, Morphology and composition controllable synthesis of Mg–Al–$CO_3$ hydrotalcites by tuning the synthesis pH and the CO 2 capture capacity, Appl. Clay Sci. 55 (2012) 18-26.

[16] Q. Song, W. Liu, C.D. Bohn, R.N. Harper, E. Sivaniah, S.A. Scott, J.S. Dennis, A high performance oxygen storage material for chemical looping processes with $CO_2$ capture, Energy Env. Sci. 6(1) (2013) 288-298.

[17] J. Plank, D. Zhimin, H. Keller, F.v. Hössle, W. Seidl, Fundamental mechanisms for polycarboxylate intercalation into C 3 A hydrate phases and the role of sulfate present in cement, Cement Concrete Res. 40(1) (2010) 45-57.

[18] A. Alcantara, P. Aranda, M. Darder, E. Ruiz-Hitzky, Bionanocomposites based on alginate–zein/layered double hydroxide materials as drug delivery systems, J. Mater. Chem. 20(42) (2010) 9495-9504.

[19] V. Rives, M. Del Arco, C. Martin, Layered double hydroxides as drug carriers and for controlled release of non-steroidal antiinflammatory drugs (NSAIDs): a review, J. Control. Release 169(1-2) (2013) 28-39.

[20] L. Li, W. Gu, J. Chen, W. Chen, Z.P. Xu, Co-delivery of siRNAs and anti-cancer drugs using layered double hydroxide nanoparticles, Biomater. 35(10) (2014) 3331-9.

[21] J.-M. Oh, S.-J. Choi, G.-E. Lee, S.-H. Han, J.-H. Choy, Inorganic drug-delivery nanovehicle conjugated with cancer-cell-specific ligand, Adv. Funct. Mater. 19(10) (2009) 1617-1624.

[22] Z. Wang, E. Wang, L. Gao, L. Xu, Synthesis and properties of $Mg_2Al$ layered double hydroxides containing 5-fluorouracil, J. Solid State Chem. 178(3) (2005) 736-741.

[23] S.A. Hindocha, L.J. McIntyre, A.M. Fogg, Precipitation synthesis of lanthanide hydroxynitrate anion exchange materials, $Ln_2(OH)_5NO_3{\cdot}H_2O$ (Ln=Y, Eu–Er), J. Solid State Chem. 182(5) (2009) 1070-1074.

[24] L.J. McIntyre, L.K. Jackson, A.M. Fogg, $Ln_2(OH)_5NO_3{\cdot}xH_2O$ (Ln= Y, Gd− Lu): A novel family of anion exchange intercalation hosts, Chem. Mater. 20(1) (2008) 335-340.

[25] L. Poudret, T.J. Prior, L.J. McIntyre, A.M. Fogg, Synthesis and crystal structures of new lanthanide hydroxyhalide anion exchange materials, $Ln_2(OH)_5X{\cdot}1.5H_2O$ (X = Cl, Br; Ln = Y, Dy, Er, Yb), Chem. Mater. 20 (2008) 7447–7453.

[26] W. Li, Q. Gu, F. Su, Y. Sun, G. Sun, S. Ma, X. Yang, Intercalation of azamacrocyclic crown ether into layered rare-earth hydroxide (LRH): secondary host-guest reaction and efficient heavy metal removal, Inorg. Chem. 52(24) (2013) 14010-7.

[27] Q. Gu, Y. Sun, N. Chu, S. Ma, Z. Jia, X. Yang, Intercalation of amino acids into $Eu^{3+}$-doped layered gadolinium hydroxide and quenching of $Eu^{3+}$ luminescence, Eur. J. Inorg. Chem. 2012(28) (2012) 4407-4412.

[28] B.I. Lee, K.S. Lee, J.H. Lee, I.S. Lee, S.H. Byeon, Synthesis of colloidal aqueous suspensions of a layered gadolinium hydroxide: a potential MRI contrast agent, Dalton Trans. (14) (2009) 2490-5.

[29] Y.-S. Yoon, B.-I. Lee, K.S. Lee, G.H. Im, S.-H. Byeon, J.H. Lee, I.S. Lee, Surface modification of exfoliated layered gadolinium hydroxide for the development of multimodal contrast agents for MRI and fluorescence imaging, Adv. Funct. Mater. 19(21) (2009) 3375-3380.

[30] F. Gándara, E.G. Puebla, M. Iglesias, D.M. Proserpio, N. Snejko, M.A. Monge, Controlling the structure of arenedisulfonates toward catalytically active materials, Chem. Mater. 21(4) (2009) 655-661.

[31] Y. Xiang, X.F. Yu, D.F. He, Z. Sun, Z. Cao, Q.Q. Wang, Synthesis of highly luminescent and anion‐exchangeable cerium‐doped layered yttrium hydroxides for sensing and photofunctional applications, Adv. Funct. Mater. 21(22) (2011) 4388-4396.

[32] Q. Zhu, J.-G. Li, C. Zhi, X. Li, X. Sun, Y. Sakka, D. Golberg, Y. Bando, Layered rare-earth hydroxides (LRHs) of $(Y_{1-x}Eu_x)_2(OH)_5NO_3{\cdot}nH_2O$ (x= 0−1): Structural variations by $Eu^{3+}$ doping, phase conversion to oxides, and the correlation of photoluminescence behaviors, Chem. Mater. 22(14) (2010) 4204-4213.

[33] B.I. Lee, S.H. Byeon, Highly enhanced photoluminescence of a rose-like hierarchical superstructure prepared by self-assembly of rare-earth hydroxocation nanosheets and polyoxomolybdate anions, Chem. Commun. 47(14) (2011) 4093-5.

[34] Q. Zhu, J.G. Li, C. Zhi, R. Ma, T. Sasaki, J.X. Xu, C.H. Liu, X.D. Li, X.D. Sun, Y. Sakka, Nanometer-thin layered hydroxide platelets of $(Y_{0.95}Eu_{0.05})_2(OH)_5NO_3{\cdot}xH_2O$: exfoliation-free synthesis, self-assembly, and the derivation of dense oriented oxide films of high transparency and greatly enhanced luminescence, J. Mater. Chem. 21(19) (2011) 6903.

[35] X. Wu, J.G. Li, Q. Zhu, J. Li, R. Ma, T. Sasaki, X. Li, X. Sun, Y. Sakka, The effects of $Gd^{3+}$ substitution on the crystal structure, site symmetry, and photoluminescence of Y/Eu layered rare-earth hydroxide (LRH) nanoplates, Dalton Trans. 41(6) (2012) 1854-61.

[36] Q. Gu, N. Chu, G. Pan, G. Sun, S. Ma, X. Yang, Intercalation of diverse organic guests into layered europium hydroxides - structural tuning and photoluminescence behavior, Eur. J. Inorg. Chem. 2014(3) (2014) 559-566.
[37] Q. Gu, F. Su, L. Ma, S. Ma, G. Sun, X. Yang, Intercalation of coumaric acids into layered rare-earth hydroxides: controllable structure and photoluminescence properties, J. Mater. Chem. C 3(18) (2015) 4742-4750.
[38] Q. Gu, F. Su, S. Ma, G. Sun, X. Yang, Controllable luminescence of layered rare-earth hydroxide composites with a fluorescent molecule: blue emission by delamination in formamide, Chem. Commun. 51(13) (2015) 2514-7.
[39] H. Kim, B.-I. Lee, H. Jeong, S.-H. Byeon, Relationship between interlayer anions and photoluminescence of layered rare earth hydroxides, J. Mater. Chem. C 3(28) (2015) 7437-7445.
[40] T. Shen, Y. Zhang, W. Liu, Y. Tang, Novel multi-color photoluminescence emission phosphors developed by layered gadolinium hydroxide via in situ intercalation with positively charged rare-earth complexes, J. Mater. Chem. C 3(8) (2015) 1807-1816.
[41] J. Key, J.F. Leary, Nanoparticles for multimodal in vivo imaging in nanomedicine, Int. J. Nanomedicine 9 (2014) 711.
[42] H. Dong, S.R. Du, X.Y. Zheng, G.M. Lyu, L.D. Sun, L.D. Li, P.Z. Zhang, C. Zhang, C.H. Yan, Lanthanide nanoparticles: From design toward bioimaging and therapy, Chem. Rev. 115(19) (2015) 10725-815.
[43] D. Stefanakis, D.F. Ghanotakis, Synthesis and characterization of gadolinium nanostructured materials with potential applications in magnetic resonance imaging, neutron-capture therapy and targeted drug delivery, J. Nanoparticle Res. 12(4) (2010) 1285-1297.
[44] Y.S. Yoon, B.I. Lee, K.S. Lee, H. Heo, J.H. Lee, S.H. Byeon, I.S. Lee, Fabrication of a silica sphere with fluorescent and MR contrasting $GdPO_4$ nanoparticles from layered gadolinium hydroxide, Chem. Commun. 46(21) (2010) 3654-6.
[45] S.S. Yoo, R. Razzak, E. Bedard, L. Guo, A.R. Shaw, R.B. Moore, W.H. Roa, Layered gadolinium-based nanoparticle as a novel delivery platform for microRNA therapeutics, Nanotechnol. 25(42) (2014) 425102.
[46] M.A. Malik, M.Y. Wani, M.A. Hashim, Microemulsion method: A novel route to synthesize organic and inorganic nanomaterials, Arabian J. Chem. 5(4) (2012) 397-417.
[47] C.J. Wang, D. O'Hare, Synthesis of layered double hydroxide nanoparticles in a novel microemulsion, J. Mater. Chem. 22(39) (2012) 21125.
[48] X. Zhang, K.-Y. Chan, Water-in-oil microemulsion synthesis of platinum-ruthenium nanoparticles, their characterization and electrocatalytic properties, Chem. Mater. 15(2) (2003) 451-459.
[49] C. Murray, D.J. Norris, M.G. Bawendi, Synthesis and characterization of nearly monodisperse CdE (E= sulfur, selenium, tellurium) semiconductor nanocrystallites, J. Am. Chem. Soc. 115(19) (1993) 8706-8715.
[50] A.J. Zarur, J.Y. Ying, Reverse microemulsion synthesis of nanostructured complex oxides for catalytic combustion, Nature 403(6765) (2000) 65-67.
[51] C.H. Lin, J.H. Chang, Y.Q. Yeh, S.H. Wu, Y.H. Liu, C.Y. Mou, Formation of hollow silica nanospheres by reverse microemulsion, Nanoscale 7(21) (2015) 9614-26.

[52] J.N. Coleman, M. Lotya, A. O'Neill, S.D. Bergin, P.J. King, U. Khan, K. Young, A. Gaucher, S. De, R.J. Smith, I.V. Shvets, S.K. Arora, G. Stanton, H.Y. Kim, K. Lee, G.T. Kim, G.S. Duesberg, T. Hallam, J.J. Boland, J.J. Wang, J.F. Donegan, J.C. Grunlan, G. Moriarty, A. Shmeliov, R.J. Nicholls, J.M. Perkins, E.M. Grieveson, K. Theuwissen, D.W. McComb, P.D. Nellist, V. Nicolosi, Two-dimensional nanosheets produced by liquid exfoliation of layered materials, Science 331(6017) (2011) 568-71.

[53] J. Rees, Synthesis, characterisation and application of layered rare-earth hydroxide nanoparticles, MChem thesis, University of Liverpool, 2012, p. 61.

[54] F. Gandara, J. Perles, N. Snejko, M. Iglesias, B. Gomez-Lor, E. Gutierrez-Puebla, M.A. Monge, Layered rare-earth hydroxides: a class of pillared crystalline compounds for intercalation chemistry, Angew. Chem. 45(47) (2006) 7998-8001.

[55] F. Geng, H. Xin, Y. Matsushita, R. Ma, M. Tanaka, F. Izumi, N. Iyi, T. Sasaki, New layered rare-earth hydroxides with anion-exchange properties, Chem. Eur. J. 14(30) (2008) 9255-60.

[56] F. Geng, Y. Matsushita, R. Ma, H. Xin, M. Tanaka, F. Izumi, N. Iyi, T. Sasaki, General synthesis and structural evolution of a layered family of $Ln_8(OH)_{20}Cl_4 \cdot nH_2O$ (Ln= Nd, Sm, Eu, Gd, Tb, Dy, Ho, Er, Tm, and Y), J. Am. Chem. Soc. 130(48) (2008) 16344-16350.

[57] Z.P. Xu, G.Q. Lu, Hydrothermal synthesis of layered double hydroxides (LDHs) from mixed MgO and $Al_2O_3$: LDH formation mechanism, Chem. Mater. 17(5) (2005) 1055-1062.

[58] G. Hu, N. Wang, D. O'Hare, J. Davis, Synthesis of magnesium aluminium layered double hydroxides in reverse microemulsions, J. Mater. Chem. 17(21) (2007) 2257.

[59] K.-H. Lee, S.-H. Byeon, Extended members of the layered rare-earth hydroxide family, $RE_2(OH)_5NO_3 \cdot nH_2O$ (RE = Sm, Eu, and Gd): Synthesis and anion-exchange behavior, Eur. J. Inorg. Chem. 2009(7) (2009) 929-936.